

Generic Model of Morphological Changes in Growing Colonies of Fungi

Juan M. López^{1,†} and Henrik J. Jensen^{2*}

¹ Instituto de Física de Cantabria, Consejo Superior de Investigaciones Científicas–Universidad de Cantabria, E-39005 Santander, Spain

² Department of Mathematics, Imperial College of Science, Technology and Medicine, 180 Queen's Gate, London SW7 2BZ, United Kingdom.

Fungal colonies are able to exhibit different morphologies depending on the environmental conditions. This allows them to cope with and adapt to external changes. When grown in solid or semi-solid media the bulk of the colony is compact and several morphological transitions have been reported to occur as the external conditions are varied. Here we show how a unified simple mathematical model, which includes the effect of the accumulation of toxic metabolites, can account for the morphological changes observed. Our numerical results are in excellent agreement with experiments carried out with the fungus *Aspergillus oryzae* on solid agar.

I. INTRODUCTION

Since the pioneering work of D'Arcy Thompson [1] at the beginning of this century understanding the origin of complex structures involving living organisms has been a challenge for physicists and biologists alike. In particular the patterns formed in growing colonies of microorganisms, like bacteria [2–7] and fungi [8–16] have attracted much interest because they exhibit properties akin to those in inanimate systems far from equilibrium [17]. Early mathematical models of fungal growth [18,19], considered fungi as purely additive assemblages of discrete individual hyphal units that duplicate at regular intervals and homogeneously. These models predict the crossover from exponential growth to linear growth of the peripheral zone as the colony matures. However, they are unable to account for many of the observable macroscopic properties (as morphological changes for instance) exhibited by fungi.

Fungal growth experiments on agar plates have shown [8–16] that filamentous growth leads to a fractal colony with patterns that have much in common with those observed in diffusion-limited aggregation (DLA) processes [20,21]. Similar branched morphologies have also been observed in bacterial growth [2–5] where the relevance of DLA was nicely demonstrated [3,4]. Sophisticated communication mechanisms, including chemotactic signals and feedback response, were later proposed [5] in order to understand the origin of branched growth in bacteria. A similar mathematical modelling might be adequate to explain the DLA-like patterns of hyphae. However, quantitative measurements of the fractal dimension of mycelia [13,8] have shown that the dimension varies in time and from one species to another. Also, the growth mechanism of DLA clusters seems rather different from the hyphal extension of fungi. Some reaction-diffusion models have also been studied [22,23], which seem to capture essential features of the filamentous fungi.

In contrast, under appropriate environmental conditions, colonies of many fungal species are also able to

display a compact phase [24,25] with uni-cellular non-cooperative growth and generate non-DLA patterns. In this case, transitions between different morphologies are also observed [14–16] when the relevant parameters in the growth conditions are varied. A mathematical model able to include all these fungal patterns on solid media has remained elusive up to now [16,26]. Here we show that a simple stochastic model containing some generic biological mechanisms is able to reproduce a variety of patterns observed in the growth of fungal colonies on solid agar plates. The model takes into account the effect of the accumulation of waste products, which play an important role as inhibitors for cell division.

Matsuura and Miyazima [14,15] carried out experiments with the fungus *Aspergillus oryzae* on agar plates of different stiffness and with different concentrations of nutrients (glucose). They observed that the fungal colonies on solid media formed a variety of shapes (see Figure 1). In nutrient-rich conditions, the colonies showed a homogeneous and smooth growth front (Fig. 1a). In contrast, growth in glucose-poor conditions resulted in colonies with rougher surfaces (Fig. 1b). The physiological ability of the fungus to divide and grow is diminished at lower temperatures [24,25], when even morphological instabilities (Fig. 1c) or an incipient branched growth (Fig. 1d) can be observed depending on the nutrient concentration. Similar patterns have recently been obtained in experiments with colonies of the yeast *Pichia membranaefaciens* on solidified agarose [16]. How can these morphological changes be qualitatively described and understood within one simple mathematical model?.

II. THE MODEL

It is known that metabolic products generated by fungal cells during the degradation of nutrients diffuse through the medium and may act as impurities inhibiting further cell division [24,25,16]. We have considered

the effect of toxic metabolites on the morphology of the colony. We have studied a model in which the growth probability at every site is coupled with an inhibitory field generated by the fungus itself. The model is defined on a two dimensional lattice as follows. At time t a lattice site can be either *occupied* by a fungal cell or *vacant*. Two quantities are assigned to every site \vec{x} in the lattice: (1) the total age of the nearest neighbour cells $A(\vec{x}, t)$ of that site and (2) the field $c(\vec{x}, t)$ containing the concentration of waste products. The spread of inhibitors from a single cell situated at \vec{x}_0 is modelled by means of a diffusion equation with a source:

$$\frac{\partial c(\vec{x}, t)}{\partial t} = D \nabla^2 c(\vec{x}, t) + s \delta(\vec{x} - \vec{x}_0) \Theta(t - \tau_0), \quad (1)$$

where Θ is the step function ($\Theta(u) = 1$ for $u \geq 0$ and $\Theta(u) = 0$ for $u < 0$). D is the diffusion constant of the metabolites, s is the inhibitor chemicals' production rate, and τ_0 is the time at which the polluting cell at \vec{x}_0 was born. The total density of waste products at any vacant site at time t is calculated by adding the contributions coming from every occupied site in colony situated within a distance d .

Colony growth occurs because of the division of individual cells, thus only nearest neighbours of occupied sites have a chance of becoming occupied. We assume that the probability for a vacant site \vec{x} of being occupied in the next time step increases with the total age $A(\vec{x}, t)$ of the occupied nearest neighbours of that vacant site \vec{x} . Therefore, at every time step, we assign a growth probability $P(\vec{x}, t)$ to every vacant site \vec{x} given by

$$P(\vec{x}, t) = F[\theta A(\vec{x}, t) \phi(c)], \quad (2)$$

which depends on the two fields $A(\vec{x}, t)$ (total age of neighbouring occupied sites) and $c(\vec{x}, t)$ (waste concentration) introduced above. In Eq.(2), F is an arbitrary monotonous increasing function satisfying $F(0) = 0$ and $F(\infty) = 1$ (properties required for P to be a probability). The results do not depend on the detailed form of F and in the following we use $F(x) = \tanh(x)$ for simplicity. The suppression of cell division due to the accumulation of metabolites is represented by $\phi(c)$ that is a decreasing function of the concentration of waste chemicals. In order to see a significant effect of the inhibitors, the decay of ϕ with c must be rapid enough. In the simulations we are presenting in this paper $\phi(c) = \exp(-c/c_0)$ was assumed, c_0 being a concentration threshold above which the effect of inhibitors becomes important. Other simple functional forms may be used and similar patterns are obtained provided that $\phi(c)$ decays rapidly enough. Finally, the external parameter θ controls directly the growth rate and is associated with the food supply (media richer in nutrients correspond to larger values of θ).

III. RESULTS

We carried out extensive simulations of the model. The simulations were performed on a two dimensional triangular lattice with open boundary conditions, simultaneously updating Eqs.(1) and (2) in every time step. The position of the front is determined and the height $h(x, t)$ at every column x is used to study the front dynamics. In order to mimic the experiments, the growth is initiated from a straight line of randomly occupied sites at $h(x, 0) = 0$. The dynamics of the growing front is characterized by the height fluctuations, which are measured by means of the front width over the total system of size L , $W(L, t) = \sqrt{\langle (h - \langle h \rangle)^2 \rangle}$. The use of other quantities to measure the width is helpful when instabilities or overhangs appear, like for instance the difference $\text{Max}[h] - \text{Min}[h]$ between the maximum and minimum heights, and gave similar results.

The model has two external parameters, namely: the growth rate θ , and the concentration threshold c_0 for inhibitory effects. These are to be thought of as effective parameters and their relation to experimental variables such as temperature, concentration of nutrients, *etc.* may not be a simple one. It is to be noted that, if experimental conditions change, for instance in such a way that the absorption of inhibitors by the fungal cells is enhanced, the effect may be well represented by either a lower threshold c_0 or a wider spread distance d (or even a combination of both).

We performed computer simulations of the model for different values of θ and c_0 . In the following we discuss the different front morphologies that are obtained depending on the values of these two parameters, and how they are related to experimental observations. In Fig. 2 we present a summary of the resulting numerical fungal patterns.

A. High threshold for inhibitory effects

The first morphological transition occurs in the limit $c_0 \rightarrow \infty$, in which the inhibitors become irrelevant ($\phi(c) \approx 1$). We found that the surface of the colony is flat (Fig. 2a) when inhibitors have little effect (for $c_0 \gg 1$) and the medium is rich in nutrients. Conversely, the growth front becomes rougher and Eden-like (Fig. 2b) for a poorer medium. In fact, a quantitative measure of the roughness (see below) indicates that the fractal dimension of the front is 1.5 [26] as in the Eden model [27]. These morphological phases are separated by a continuous phase transition at a critical value of $\theta = \theta_c$. For large growth rates (rich medium) $\theta > \theta_c$ the front is flat, $W \sim \text{const}$. In contrast, if the growth rate is reduced below θ_c (poor medium) the front becomes rougher and exhibits the dynamical scaling behaviour typical of a scale-free roughening process [28,27]. As can be seen in Fig. 3, in the rough phase the width grows like a power

law $W \sim t^\beta$ until a stationary regime is reached and $W \sim L^\alpha$, where L is the system size. Our determination of the time exponent $\beta = 0.24 \pm 0.02$ and the roughness exponent $\alpha = 0.46 \pm 0.05$ indicates that the model belongs to the Edwards-Wilkinson universality class [29] in this phase. The computation of the roughness exponent α allows us to determine the fractal dimension D_f of the front through the relation $D_f = 2 - \alpha \simeq 1.54$, which is consistent with Eden-like growth. This morphological transition from rough to flat growth has recently been studied in detail by us [26] for a much simpler version of this model, which corresponds to the limit $c_0 \rightarrow \infty$. We found that $\theta_c = 0.183 \pm 0.003$ in the limit case of $c_0 = \infty$. When approaching the roughening transition from the rough phase ($\theta < \theta_c$) to the flat phase ($\theta > \theta_c$), a diverging correlation length $\xi \sim |\theta - \theta_c|^{-\nu}$ appears. The critical exponent was found to be $\nu = 1.10$. At the phase transition the scaling exponents can be calculated by mapping the problem onto directed percolation (see Ref. [26] for further details). Experimental realizations of transitions from a flat to a rough front can be observed in the Matsuura and Miyazima experiments shown in Figure 1a-1b. As our model predicts the richer the medium the flatter the front.

B. Low threshold for inhibitory effects

If the effect of toxic inhibitors on the fungus is enhanced, further interfacial instabilities in the front appear. Lower temperatures are less favorable for the physiological activity of the fungus [24,25] and its capacity to divide. One can model this effect by a smaller threshold c_0 for the inhibition of cell division. One can observe (Fig. 2c) that, as c_0 is decreased, deep grooves and overhangs develop in the colony and some regions with high concentration of inhibitors are eventually surrounded by the colony front. The presence of an unstable growth dynamics can be realized by the appearance of an extremely rapid (exponential) growth of the interface width $W(L, t)$ in this regime, as shown in Fig. 4. This regime is to be compared with the patterns observed in the experiments (Fig. 1c).

Finally, in the worst of the situations, the growth becomes very localized and only the dominant filaments branch out into the empty medium (Fig. 2d). This is due to the building up of extremely high concentrations of waste products in some regions that the fungus cannot invade any longer. There is qualitative agreement with the experiment shown in Fig. 1d.

The four major morphological phases are summarized in the qualitative phase diagram in Fig. 5. The solid line that separates the rough from the flat phase in Fig. 5 has recently been shown to be a nonequilibrium continuous phase transition and can be mapped into directed percolation [26]. However, we were unable to find a sharp transition between the remaining phases.

IV. DISCUSSION

Our results indicate that the morphologies generated during the growth of fungal colonies on solid agar can be modeled by taking into account (1) the building up of a concentration of waste inhibitors in the medium and (2) the provision of nutrients. We have studied a simple model which allows us to understand the interplay between these two mechanisms. The morphological transformations that we have found can be compared with recent experiments on pattern formation in fungal growth.

In our model, a constant growth rate θ has been assumed. The effect of the exhaustion and diffusion of nutrients can be modeled by replacing θ by a diffusive field, which is depleted at a certain rate at sites occupied by fungal cells. This would have a major impact on the front dynamics as the front will eventually stop growing because of agar exhaustion.

Our model approach to pattern formation in fungal colony growth is stochastic and includes in a natural way the random nature of cell division. This together with the accumulation of inhibiting chemicals produces some of the different morphological phases observed in experiments. This is in contrast to other existing models based upon non-linear diffusion, in which evolution is deterministic and patterns arise from nonlinear instabilities. They represent a different level of description of the same phenomena. Both type of models coexist at different levels of description.

Finally, while our model can account for the morphological changes observed in some fungi growing in agar culture, we should mention that this model may not be appropriate for describing the morphological patterns observed in other fungal species. Our results compare well with the fungus *Aspergillus oryzae* which, like many members of this genus (and also the genus *Penicillium*), form dense colonies that expand only very slowly and seem to be self-inhibitory.

The authors are in debt to S. Matsuura for kindly providing us photographs of their experiments. We thank T. Sams for useful discussions on his work and M.J. Carlile, S. Matsuura, and E. Calle for helpful comments and correspondence. This work has been supported by a grant from the European Commission (Contract No. HPMF-CT-99-00133)).

[†] Electronic address: lopez@ifca.unican.es

^{*} Electronic address: h.jensen@ic.ac.uk

[1] D'Arcy Thompson, *On Growth and Form*, Cambridge University Press (1997), reprint of the 1917's original version.

[2] A.L. Cooper *et. al.*, Proc. Roy. Soc. Lond. B **175**, 95 (1970).

[3] H. Fujikawa and M. Matsushita, J. of Phys. Soc. Jpn. **58**, 3875 (1989).

[4] M. Matsushita and H. Fujikawa, Physica A **168** 498 (1990).

[5] E. Ben-jacob *et. al.*, Nature **368**, 46 (1994).

[6] T. Matsuyama and M. Matsushita in P.M. Iannaccone and M. Khokha Eds., *Fractal Geometry in Biological Systems*, CRS Press Inc., Florida (1996).

[7] E. Ben-Jacob, Contem. Phys. **38**, 205 (1997).

[8] M. Obert *et. al.*, J. Bacteriology **172**, 1180 (1990).

[9] C.L. Jones *et. al.*, Binary **5**, 171 (1993).

[10] J.D. Mihail, *et. al.*, Mycol. Res. **99**, 81 (1995).

[11] R.G. Bolton and L. Boddy, Mycol. Res. **97**, 762 (1993).

[12] D.P. Donnelly, D.P. Wilkins and L. Boddy, Binary **7**, 19 (1995).

[13] K. Ritz and J. Crawford, Mycol. Res. **94**, 1138 (1990).

[14] S. Matsuura and S. Miyazima, Physica A **191**, 30 (1992).

[15] S. Matsuura and S. Miyazima, Fractals **1**, 11 (1993).

[16] T. Sams *et. al.*, Phys. Rev. Lett. **79**, 313 (1997).

[17] E. Ben-Jacob and P. Garik, Nature **343**, 523 (1990).

[18] A.P.J. Trinci in *The filamentous fungi*, vol.3, *Developmental mycology*, J.E. Smith and D.R. Berry, eds., E. Arnold, London (1978).

[19] J.I. Prosser in *The Growing Fungus*, N.A.R. Gow and G.M. Gadd, eds., Chapman & Hall, London (1995).

[20] T.A. Witten and L.M. Sander, Phys. Rev. Lett. **47**, 1400 (1981).

[21] L.M. Sander, Nature **322**, 789 (1986).

[22] C.M. Regalado *et. al.*, Mycol. Res. **100**, 1473 (1996).

[23] F.A. Davidson *et. al.*, Proc. R. Soc. Lond. B **263**, 873 (1996).

[24] N.A.R. Gow and G.M. Gadd, eds. *The Growing Fungus*, Chapman & Hall, London (1995).

[25] M.J. Carlile and S.C. Watkinson, *The Fungi*, Academic Press, London (1994).

[26] J.M. López and H.J. Jensen, Phys. Rev. Lett. **81**, 1734 (1998).

[27] F. Family and T. Vicsek (eds.), *Dynamics of Fractal Surfaces*, World Scientific, Singapore (1991).

[28] A.-L. Barabási and H. E. Stanley, *Fractal Concepts in Surface Growth*, Cambridge University Press, Cambridge (1995).

[29] S. F. Edwards and D. R. Wilkinson, Proc. R. Soc. London A **381**, 17 (1982).

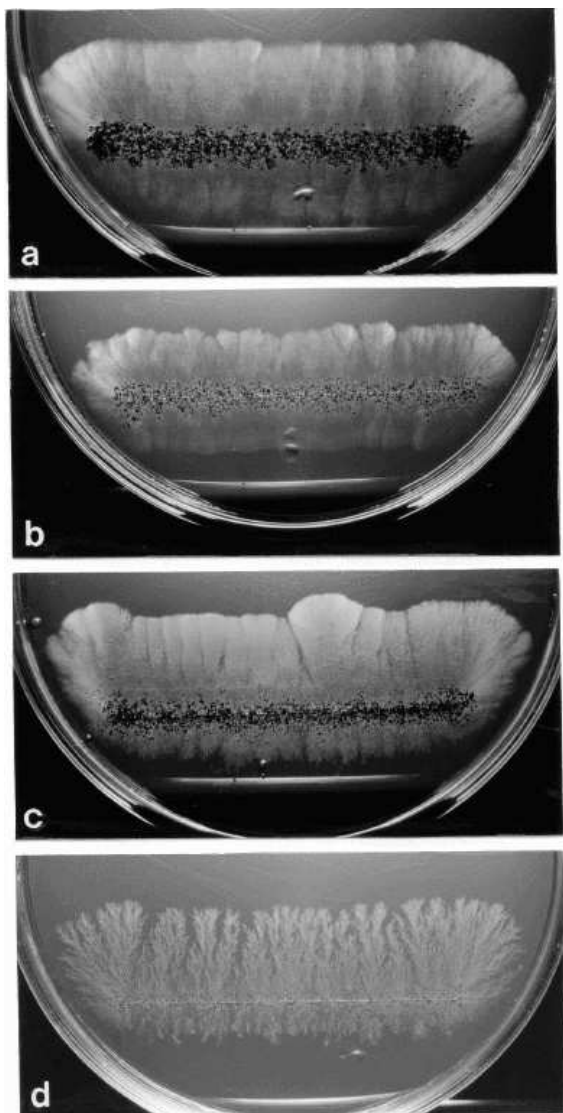


FIG. 1. Observed patterns of colonies of *Aspergillus oryzae* grown on solid medium (1.5 wt% of a Czapek synthetic agar in 25 ml of sterile medium). Experiments were carried out in media with two different concentrations of nutrients: 0.1 wt% glucose for a nutrient-rich medium and 0.01 wt% glucose in nutrient-poor conditions. (a) Smooth colony 10 days after inoculation at 24°C in a nutrient-rich medium; (b) patterns 8 days after inoculation at 24°C in a poor medium, where the colony developed a rough front. (c) 30 days at 18°C in a rich medium. Note the tip splitting dynamics and groovy structure of the colony associated with the existence of a morphological instability. (d) Prominent filamentous patterns of a colony grown in a nutrient-poor medium after 35 days at 18°C . Photographs kindly provided by S. Matsuura.

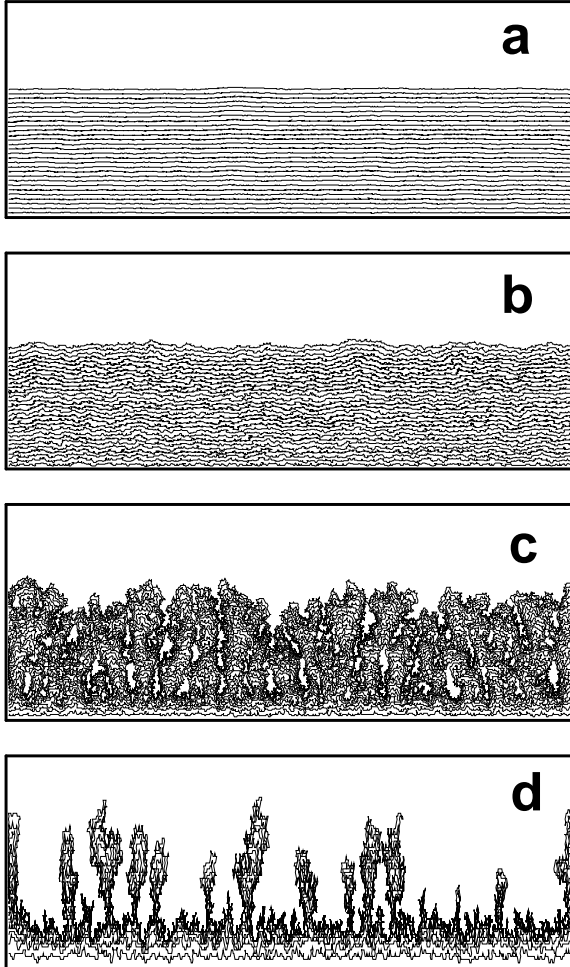


FIG. 2. Fungal patterns obtained by numerical simulation of the model on a triangular lattice of lateral size $N = 500$. Each front corresponds to the position of the colony surface at equal time intervals. When the threshold c_0 is large ($c_0 = 5.0$), two different morphologies appear: (a) the colony is flat in a nutrients-rich medium, $\theta = 0.1$ and (b) rough in the nutrients-poor case, $\theta = 0.01$. For small values of the threshold c_0 , the colony exhibits a morphological instability as in (c) for $c_0 = 1.0$; or prominent filamental growth as in (d) for $c_0 = 0.7$. In the simulations shown, the production rate of toxic metabolites and the diffusion constant are fixed to $s = 0.05$ and $D = 1$ respectively. Sites within a distance $d = 16$ are considered to calculate the concentration of inhibitors at any site.

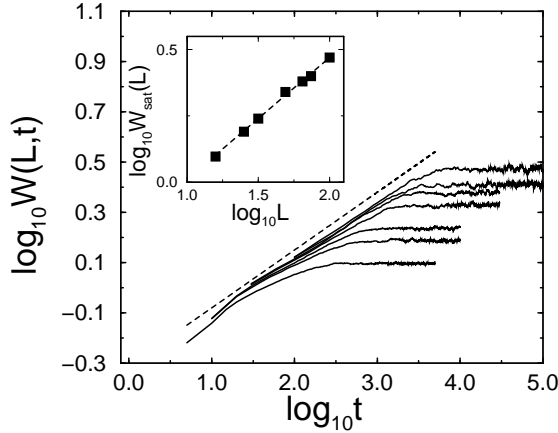


FIG. 3. Interface width of the front *vs.* time in the rough phase ($\theta = 0.01$) for different system sizes $L = 16, 25, 32, 50, 64, 75, 100$. The slope of the dotted line corresponds to the time exponent $\beta = 0.24 \pm 0.02$. In the inset the values of the width at saturation are plotted *vs.* system size. The dotted line fits the data and gives the roughness exponent $\alpha = 0.46 \pm 0.05$.

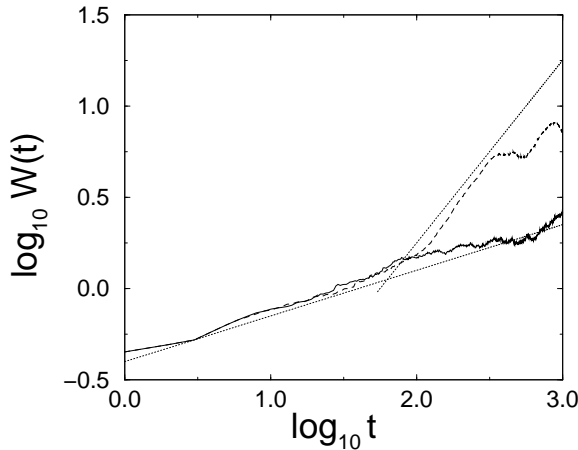


FIG. 4. Time behaviour of the interface width in the rough (solid line) and unstable phases (dashed line). Note the change from power law behaviour $W(t) \sim t^\beta$ to exponential growth $W(t) \sim \exp t$ in the unstable case. The lines are to guide the eye and have slopes 0.25 and 1. The system size was $L = 500$. The external parameters are $\theta = 0.01$ and $c_0 = 5$ (rough phase) and $\theta = 0.01$ and $c_0 = 1$ (grooves' phase), corresponding to Figs. 2b and 2c respectively.

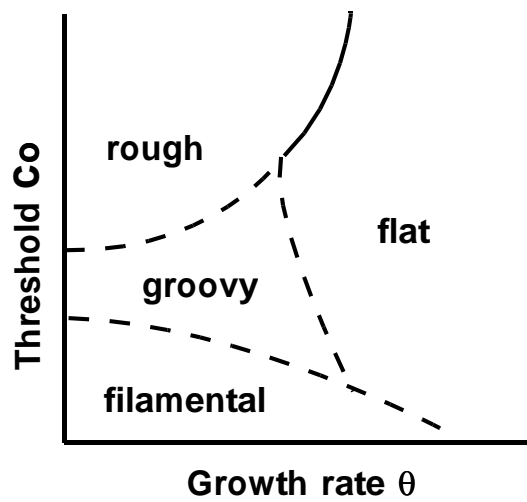


FIG. 5. Sketch of the phase diagram showing the different morphologies observed in the model. The solid line corresponds to the continuous phase transition studied in Ref.[26].